

A Role for 2-Methyl Pyrrole in the Browning of 4-Oxopentanal and Limonene Secondary Organic Aerosol

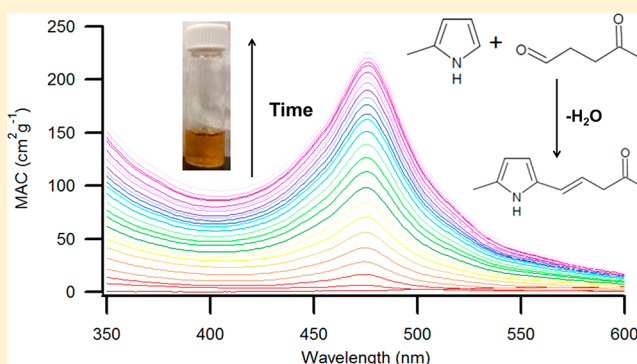
Paige K. Aiona,[†] Hyun Ji Lee,[†] Peng Lin,[‡] Forrest Heller,[§] Alexander Laskin,[‡] Julia Laskin,[‡] and Sergey A. Nizkorodov^{*,†}

[†]Department of Chemistry, University of California, Irvine, California 92697, United States

[‡]Department of Chemistry, Purdue University, West Lafayette, Indiana 47907, United States

[§]Environmental Molecular Science Laboratory, Energy and Environment Directorate, Pacific Northwest National Laboratory, Richland, Washington 99354, United States

ABSTRACT: Reactions of ammonia or ammonium sulfate (AS) with carbonyls in secondary organic aerosol (SOA) produced from limonene are known to form brown carbon (BrC) with a distinctive absorption band at 505 nm. This study examined the browning processes in aqueous solutions of AS and 4-oxopentanal (4-OPA), which has a 1,4-dicarbonyl structural motif present in many limonene SOA compounds. Aqueous reactions of 4-OPA with AS were found to produce 2-methyl pyrrole (2-MP), which was detected by gas chromatography. While 2-MP does not absorb visible radiation, it can further react with 4-OPA eventually forming BrC compounds. This was demonstrated by reacting 2-MP with 4-OPA or limonene SOA, both of which produced BrC with absorption bands at 475 and 505 nm, respectively. The formation of BrC in the reaction of 4-OPA with AS and ammonium nitrate was greatly accelerated by evaporation of the solution suggesting an important role of the dehydration processes in BrC formation. 4-OPA was also found to produce BrC in aqueous reactions with a broad spectrum of amino acids and amines. These results suggest that 4-OPA may be the smallest atmospherically relevant compound capable of browning by the same mechanism as limonene SOA.



1. INTRODUCTION

Atmospheric particles have a significant direct effect on the global radiative budget due to scattering and absorption of solar radiation and an indirect effect due to modification of cloud properties.¹ Light scattering by particles is the dominant direct effect, resulting in a negative forcing on climate (cooling). Light absorption reduces the cooling effect of particles by transforming a fraction of the solar energy into trapped heat.^{2–4} There is an uncertainty in the sign and magnitude of the overall radiative forcing by aerosols^{1,2} because a majority of atmospheric particles scatter radiation, but a highly variable fraction of light-absorbing particles, namely mineral dust, black carbon, and brown carbon, have the ability to reduce the cooling effect of aerosols.^{5–11}

Brown carbon (BrC) refers to light-absorbing carbonaceous matter in atmospheric particles capable of absorbing visible and near-UV radiation.^{6,12} BrC is attributed to primary sources, such as emissions from combustion and biomass burning, as well as secondary formation through multiphase chemistry involving particles, cloud microdroplets, and gases during atmospheric aging.^{5–7,13} Secondary sources of BrC include: OH oxidation of aromatic hydroxyacids and phenols in cloudwater,^{14–16} reactive uptake of gaseous isoprene and its derivatives on acidic atmospheric particles,^{17,18} aqueous

photochemistry of pyruvic acid in the presence of common atmospheric electrolytes,^{19,20} acid-catalyzed aldol condensation of volatile aldehydes,^{21–28} nitration of polycyclic aromatic hydrocarbons,^{29–31} and formation of secondary organic aerosol (SOA) on highly acidic seed particles.^{17,32} Secondary BrC can also be formed by the reactions of carbonyls with aqueous NH_4^+ , amino acids, and gaseous ammonia. For example, aqueous and multiphase reactions of 1,2-dicarbonyls (glyoxal and methylglyoxal) with ammonium sulfate (AS) or amino acids have been found to produce BrC.^{33–44}

Particular interest has been given to secondary BrC formed by the reaction of SOA with ammonia (NH_3) or AS, which may occur in geographic areas with large emissions of NH_3 . SOA formed by the ozonolysis of limonene (LSOA) was found to be surprisingly effective in producing BrC by this mechanism,^{45–50} in stark contrast with SOA formed by ozonolysis of α -pinene.⁵¹ This aging process results in minor changes in the overall chemical composition of SOA, but a dramatic change in optical properties due to chromophores that give BrC its

Received: May 3, 2017

Revised: August 30, 2017

Accepted: August 31, 2017

Published: August 31, 2017

color.^{45,47,48,51,52} Nguyen et al. (2013) investigated possible precursors responsible for the production of these chromophores in LSOA, specifically pinonaldehyde, limonoaldehyde, and ketolimononaldehyde (KLA). It was found that KLA, a secondary product of limonene ozonolysis, was the only precursor to produce brown products upon exposure to reduced nitrogen compounds, demonstrating a remarkable sensitivity of this process to the molecular structure of the precursor.⁵²

The mechanism for the production of BrC chromophores via NH₃-mediated aging is actively being investigated.¹² It has been proposed that carbonyls react with NH₃ to form primary amines, which then undergo further reactions with unreacted carbonyls to form more stable secondary amines.^{51,52} These reactions are reversible, with the equilibrium shifted toward the carbonyl reactants. However, in the presence of multiple carbonyl groups within the same molecule, intramolecular cyclization may occur to form a stable *N*-heterocyclic compound. For example, formation of pyrrole-based compounds was recently observed in reaction of 1,4-dicarbonyl compound 2,5-hexanedione with AS or glycine.⁵³ The *N*-heterocyclic compounds can then undergo intermolecular carbonyl-imine condensation reactions to form the larger, conjugated oligomers.⁵¹

While the general features of the reaction mechanism are established, the molecular structures of the actual chromophores have not been determined. Even in the case of a single KLA precursor reacting with NH₃, a number of products were observed and the structures of the chromophores could not be confidently assigned.⁵² Therefore, it is important to identify simpler model systems that lead to browning by closely related mechanisms. This study attempts to simplify the search for BrC chromophores by focusing on the 1,4-dicarbonyl substructure of KLA, using 4-oxopentanal (4-OPA) as a representative model system. To highlight the importance of the aldehyde group in 4-OPA we also examined a structurally related compound 6-methyl-hepten-2-one (6-MHO), which differs from 4-OPA by the lack of the reactive aldehyde group (Figure 1). 6-MHO is often coproduced with 4-OPA in the environment. For example, squalene, a compound commonly

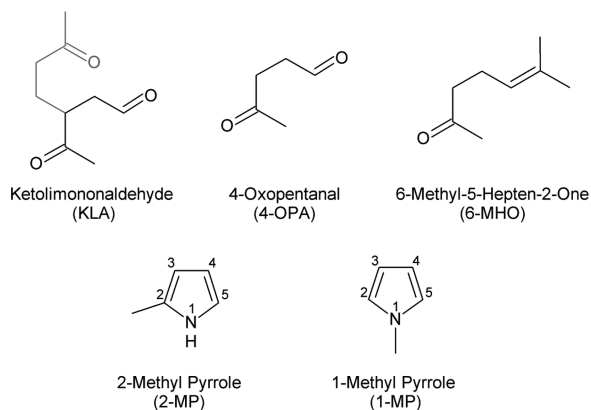


Figure 1. Structures of ketolimononaldehyde (KLA), 4-oxopentanal (4-OPA), 6-methyl-5-hepten-2-one (6-MHO), 2-methyl pyrrole (2-MP), and 1-methyl pyrrole (1-MP). KLA is a known BrC precursor. A portion of its structure is shown in gray to emphasize the structural similarity between KLA and 4-OPA. The browning potential of 4-OPA and 6-MHO are tested in this work, while 2-MP and 1-MP are investigated as possible reaction intermediates.

found in plant and animal lipids, undergoes ozonolysis to form 6-MHO as a primary product and 4-OPA as a secondary product.⁵⁴ Both 6-MHO and 4-OPA can also be produced via oxidation of common fragrance compounds, such as limonene, α -terpineol, and geraniol, with ozone or the hydroxyl radical.⁵⁵ The presence of 6-MHO and 4-OPA in the atmosphere has been confirmed in several field studies.^{56–59} Additionally, the reaction of ozone with human skin lipids has been found to produce 6-MHO and 4-OPA in indoor environments at concentrations that may be hazardous to human health.^{60,61}

In this work, we show that the reaction of 4-OPA with AS results in carbonyl-imine conversion of the aldehyde group, followed by intramolecular cyclization to form a 2-methyl pyrrole (2-MP) intermediate, as shown in Figure 2. The

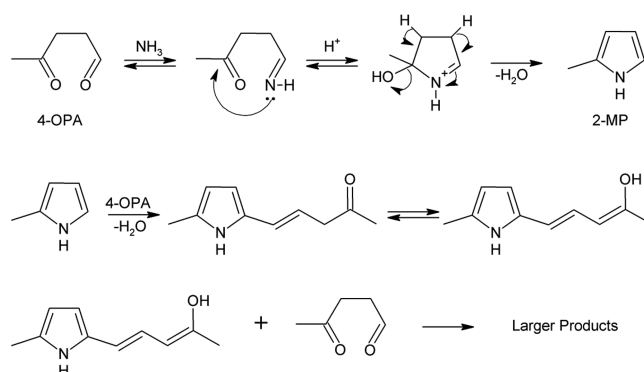


Figure 2. (Top) 4-OPA reacting with NH₃ to form 2-MP, an intermediate to the production of BrC chromophores. (Bottom) 2-MP further reacting with 4-OPA to form dimer products. A series of such reactions can produce larger, conjugated products potentially capable of absorbing visible light.

proposed mechanism is consistent with the work of Kampf et al. (2016), who observed pyrrole derivative in reactions 2,5-hexanedione with AS.⁵³ The resulting 2-MP further reacts with 4-OPA to form oligomerization products, such as the dimer shown in Figure 2 (the identification of the actual chromophoric products will be described in a follow-up paper).

To confirm this hypothesis, we carried out bulk aqueous phase studies of 4-OPA mixed with AS or with 2-MP. Control experiments were also done using 6-MHO instead of 4-OPA and 1-methyl pyrrole (1-MP) instead of 2-MP, in order to examine molecular selectivity of this browning mechanism. The browning in 4-OPA + AS mixtures and lack of browning in 6-MHO + AS mixtures confirmed the importance of the presence of both carbonyl groups in 4-OPA. In addition, we found that browning in 4-OPA + AS and LSOA + AS aqueous mixtures leads to similar types of chromophores with distinctive absorption bands in the visible spectrum. Experiments were also done to examine acceleration in browning reactions during the evaporation of water in comparison to those undergoing slow aging in solution; a phenomenon that has been observed in the LSOA + AS BrC systems.⁴⁶ Lastly, 4-OPA reacting with a broad range of amino acids and amines resulted in the formation of BrC. We conclude that 4-OPA may be the smallest atmospherically relevant compound capable of browning by the same mechanism as LSOA, and a convenient model system for studying secondary BrC formation.

2. EXPERIMENTAL METHODS

2.1. Aqueous Phase Reactions of 4-OPA with AS, 2-MP, and 1-MP. Experiments were performed to examine slow aging of aqueous phase 4-OPA in AS solution as a function of time. Liquid 4-OPA (>98% purity) was custom synthesized by commercial vendors DevirChim, Inc. (Roissy, France) and Richman Chemical Inc. (Lower Gwynedd, PA). Solutions of AS were made by dissolving solid AS (Fisher Scientific, $\geq 99\%$) in deionized water. The reaction was initiated by adding a desired amount of 4-OPA to the AS solution and placing the mixture in a 1 cm quartz cuvette with a sealed top at room temperature ($\sim 23\text{ }^\circ\text{C}$). UV-vis spectra ranging from 200 to 700 nm were recorded every 1–2 h to monitor the progress of reaction for 36 to 100 h, using a Shimadzu 1800 spectrophotometer with a distilled water reference. The three concentration combinations of 4-OPA in AS were: 0.2 M 4-OPA in 0.1 M AS, 0.06 M 4-OPA in 0.1 M AS and 0.03 M 4-OPA in 0.06 M AS. The UV-vis experiments were repeated with 6-MHO (Sigma-Aldrich, 99%), a known precursor of 4-OPA in the atmosphere, to determine whether the aldehyde group of 4-OPA, which is absent in 6-MHO (Figure 1), is required for browning.

In order to positively confirm the formation of the 2-MP intermediate in the browning reaction, the 4-OPA + AS mixture was extracted with dichloromethane, and the brown extract was analyzed by gas chromatography electron impact ionization mass spectrometry (GC-EI-MS). A 2-MP standard in dichloromethane was analyzed as well and compared to samples taken from the 4-OPA + AS reaction mixture.

2-MP (Ark Pharm Inc., >95%) or 1-MP (Sigma-Aldrich, 99%) were used in place of AS to determine whether browning can occur through reactions with the 2-MP intermediate, without direct involvement of AS, and to determine whether the placement of the methyl group on the pyrrole ring has an influence on browning. Concentrations of 4-OPA and MP were: 0.2 M 4-OPA in 0.1 M 1-MP or 2-MP and 0.06 M 4-OPA in 0.1 M 2-MP. The initial aqueous mixtures were opaque due to the presence of a colloid. To keep the reactants and products dissolved, 1 mL of each mixture and 1 mL of acetonitrile were combined, resulting in a transparent solution (implying that the reaction products were more soluble in acetonitrile than in water). The measurements were done with a Shimadzu 2450 spectrophotometer collecting a spectrum every 15–30 min over 5–24 h while stirring and water cooling at $20\text{ }^\circ\text{C}$ to minimize acetonitrile evaporation.

In order to compare the results with a previously studied LSOA + AS system,⁴⁷ LSOA was generated in a 14 L flow tube by a gas-phase reaction between limonene and ozone. Liquid limonene was injected into 5 SLM (standard liters per minute) air flow via a syringe pump at a rate of $25\text{ }\mu\text{L/h}$. Ozone produced by flowing oxygen (Airgas; 99.994%) through an ozone generator at 0.7 SLM was injected downstream of the limonene injection. The initial mixing ratios of the limonene and ozone were 11 and 9 ppm respectively, and the flow tube residence time was 2.5 min. The aerosol exited the flow tube, passed through a charcoal filter to remove excess ozone, and was collected on a foil substrate using a Sioutas Cascade Impactor. Several milligrams of LSOA were collected and dissolved in 1:1 acetonitrile in nanopure water to achieve a mass concentration comparable to the 0.06 M 4-OPA solution. The resulting solution was mixed with 0.1 M 2-MP and allowed to react. The UV-vis spectra of the LSOA + 2-MP sample were recorded every 15 min for 22 h.

2.2. Reactions of 4-OPA in Evaporating Solutions. The combination of 0.06 M 4-OPA + 0.1 M AS was selected to examine the possible acceleration of the browning process by evaporation. Solutions were mixed in a scintillation vial to create a total mixture volume of 2 mL. The vial was connected to a Buchi Rotavapor R-215 at $30\text{ }^\circ\text{C}$ and evaporated under rough vacuum ($<10\text{ mbar}$) for 10 min until all of the water was removed and only a brown residue remained. Subsequently, 2 mL of distilled water was added to the vial to dissolve the residue and a UV-vis spectrum of the resulting solution was acquired. This evaporation and dissolving process was repeated three times, until the change in the measured absorbance was minimal. Similar evaporation experiments were done with ammonium nitrate (AN; Fisher Scientific, $\geq 99\%$) in place of AS for comparison. A control experiment was also done in the absence of ammonium ions, by evaporating the solution of 4-OPA alone. The UV-vis spectra obtained in this set of evaporation experiments were compared to the spectrum acquired for the aqueous 0.06 M 4-OPA + 0.1 M AS sample aged for 48 h at room temperature.

2.3. Reactions of 4-OPA with Amines and Amino Acids. Additional studies were performed to investigate the reactions of 4-OPA with a variety of other reduced-nitrogen species, including amines, amides, and nitroso compounds. The reagents were purchased from Sigma-Aldrich at the highest available purities (typically >98%) and used without further purification. Based on qualitative observations, only certain amines formed brown products while the amides (acetamide, *N,N*-dimethylacetamide, *N,N*-dimethylformamide) and *N*-nitrosodiethylamine did not. In order to quantitatively test the amines and compare them to reactions with ammonia, stock solutions of 0.09 M were prepared using the following reagents: 2-amino-2-methyl-1-propanol (AMP), AS, diethylamine (DEA), dimethylamine (DMA), ethylenediamine (EDA), glycine (GLY), methylamine (MA), methyldiethanolamine (MDEA), ethanolamine (MEA), ammonium hydroxide (NH_4OH), AN, propylamine (PA), piperazine (PIP), and trimethylamine (TMA). A stock solution of 0.03 M 4-OPA was also prepared. A fixed volume of 4-OPA stock solution and varying volume fractions of nitrogen-containing stock solutions were mixed together and diluted to a total volume of 1.0 mL, resulting in 0.015 M 4-OPA and 0.0–0.045 M nitrogen-containing compound. The UV-vis spectrum of the initial mixture was recorded with a UV-vis spectrophotometer (USB 2000+, Ocean Optics). Each sample was aged at an elevated temperature of $40\text{ }^\circ\text{C}$ to increase the reaction rate. After a 75 min interval, the sample was removed from the incubator and its UV-vis spectrum was recorded. The procedure was repeated until the observed absorption spectrum stopped changing.

2.4. Mass Absorption Coefficient (MAC). The effective mass absorption coefficient (MAC) was used to quantify the extent of browning in all studied mixtures. The MAC was calculated using the base-10 absorbance A_{10} of the sample with the total organic carbon mass concentration of the solution C_{mass} (g cm^{-3}) and the path length of the cuvette b (cm):⁶²

$$\text{MAC}(\lambda) = \frac{A_{10}(\lambda) \times \ln(10)}{b \times C_{\text{mass}}} \quad (1)$$

C_{mass} was the mass concentration of the carbonyl reactant (4-OPA, 6-MHO or LSOA). The change in the mass of organics resulting from the ammonia reaction is minor based on results

of previous studies of KLA⁵² and LSOA.⁵¹ GC-EI-MS experiments confirmed that only a small fraction of 4-OPA was converted into BrC products. Therefore, the nitrogen-containing reactants (AS, AN, 2-MP, 1-MP, amino acids, amines, etc.) were not included in C_{mass} to make it easier to compare results of different experiments. For aqueous reactants (4-OPA and 6-MHO), C_{mass} was calculated by converting the measured volume of the reactant to mass using its density and dividing it by the total volume of solution. For LSOA, the mass of SOA on the filter was divided by the volume of solvent used for extraction.

3. RESULTS AND DISCUSSION

3.1. Role of Pyrrole Compounds in Browning Reactions of 4-OPA and LSOA with AS. Figure 3a shows time-dependent MAC spectra for a mixture containing 0.06 M 4-OPA and 0.1 M AS. In this mixture, as well as all other 4-OPA in AS mixtures examined in this work, a well-defined absorption peak at 475 nm increased in intensity as time progressed, accompanied by a visible browning of the solutions. The initial growth rate of the 475 nm peak increased with the concentration of 4-OPA and AS in solution (Figure 3c). However, the extent of browning at longer time scales did not correlate with 4-OPA concentration.

LSOA was also mixed with AS and aged in a similar way, resulting in browning of the solution as observed in previous experiments.⁴⁵ Figure 3b compares the MAC spectra of the aged 4-OPA + AS and LSOA + AS solutions after 22 h. Both systems generated prominent absorption peaks at similar wavelengths (475 nm for 4-OPA and 505 nm for LSOA) and with comparable MAC values. These results suggest that browning of 4-OPA and LSOA occurs by a similar mechanism. In addition, these results support our assumption that the 1,4-dicarbonyl motif of KLA contributes to the browning of LSOA.⁵² The shift of the 505 nm peak in the LSOA + AS system to 475 nm in the 4-OPA + AS system may be due to the smaller molecular size of chromophores formed in the latter system. LSOA is a rather complex mixture of different compounds, which contains molecules with structurally similar motifs to 4-OPA, but also with other functional groups that may lead to the observed spectral shift. Mixtures of 6-MHO with AS did not produce a significant growth of new bands in the absorption spectra. This confirms that the aldehyde group in 4-OPA, which is absent in 6-MHO, is required for browning to occur, further supporting the assumption in Figure 2 that both carbonyl groups in 4-OPA are essential for its browning chemistry.

Our hypothesis is that browning begins by reaction of 4-OPA with dissolved NH_3 resulting in the formation of a 2-MP intermediate after intramolecular cyclization. Formation of more complex compounds (Figure 2), some of which may be light absorbing, is initiated by oligomerization reactions between 2-MP with 4-OPA. To prove that 2-MP is actually produced in the 4-OPA + AS aqueous reaction, we compared the GC-MS chromatograms of the reaction mixture with that of a 2-MP solution in dichloromethane. The 2-MP standard eluted at 3.8 min and had three distinct peaks in the EI mass spectrum, at m/z 53, 80 and 81, in agreement with the mass spectrum of 2-MP in the NIST library. 4-OPA eluted at 4.1 min and had strong peaks at m/z 57, 72, and 85, as well as a number of weaker peaks, including one at m/z 81 (but no peak at m/z 80). A selected ion chromatogram for the extracted 4-OPA + AS mixture observed at m/z 80 produced a chromatographic

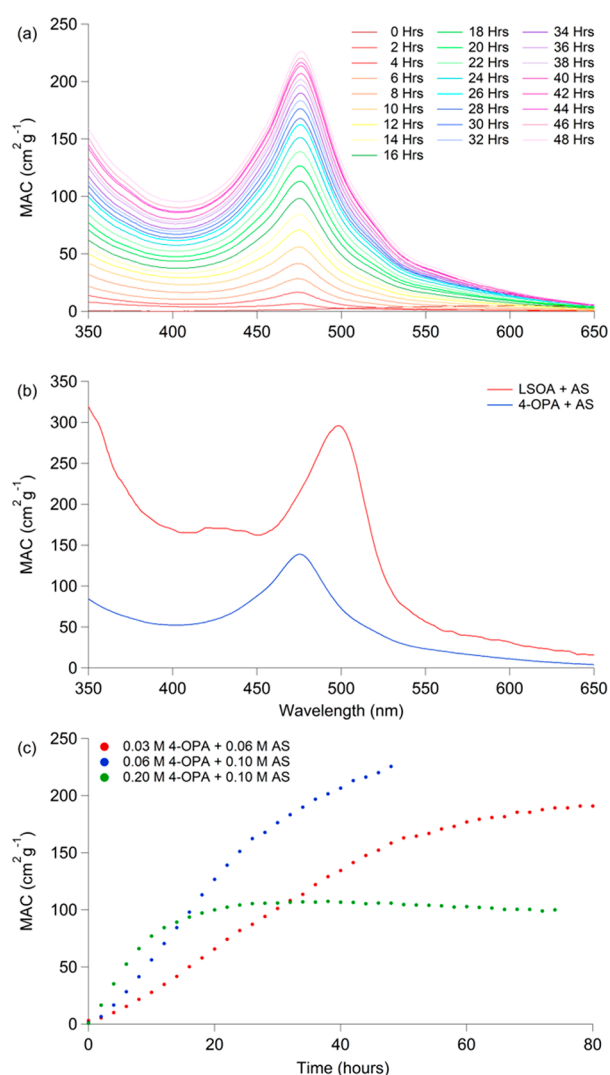


Figure 3. (a) Time-dependent MAC of 0.06 M 4-OPA in 0.1 M AS showing the growth of an absorption peak at 475 nm, accompanied by browning of the solution. (b) A comparison of MAC spectra for 4-OPA and LSOA after slow aging with AS for 22 h. (c) Comparison of peak growth at 475 nm for each combination of 4-OPA + AS concentrations tested.

peak at the same retention time (3.8 min) as in the 2-MP standard. In addition to the unreacted 4-OPA and 2-MP, the mixture contained a number of other compounds eluting between 2 and 30 min, suggesting complex secondary chemistry leading to BrC formation. None of these compounds could be identified using the NIST mass spectral library.

To further demonstrate the important role of 2-MP in browning of 4-OPA, we acquired UV-vis spectra of 0.2 M 4-OPA and 0.06 M 4-OPA in 0.1 M 2-MP mixtures. Figure 4a shows results of the 0.2 M 4-OPA + 0.1 M 2-MP experiment, in which a peak growth occurs at 475 nm, a wavelength pertinent to the browning of 4-OPA + AS mixtures. Browning was found to occur more quickly at 0.2 M in comparison to 0.06 M 4-OPA. To investigate the importance of methyl group placement on the pyrrole ring, 0.2 M 4-OPA was reacted with 0.1 M 1-MP in place of 2-MP. The mixture of 4-OPA and 1-MP did not produce absorption peaks in the visible range (Figure 4b), indicating that the formation of light-absorbing products is sensitive to the position of the methyl group in the pyrrole ring

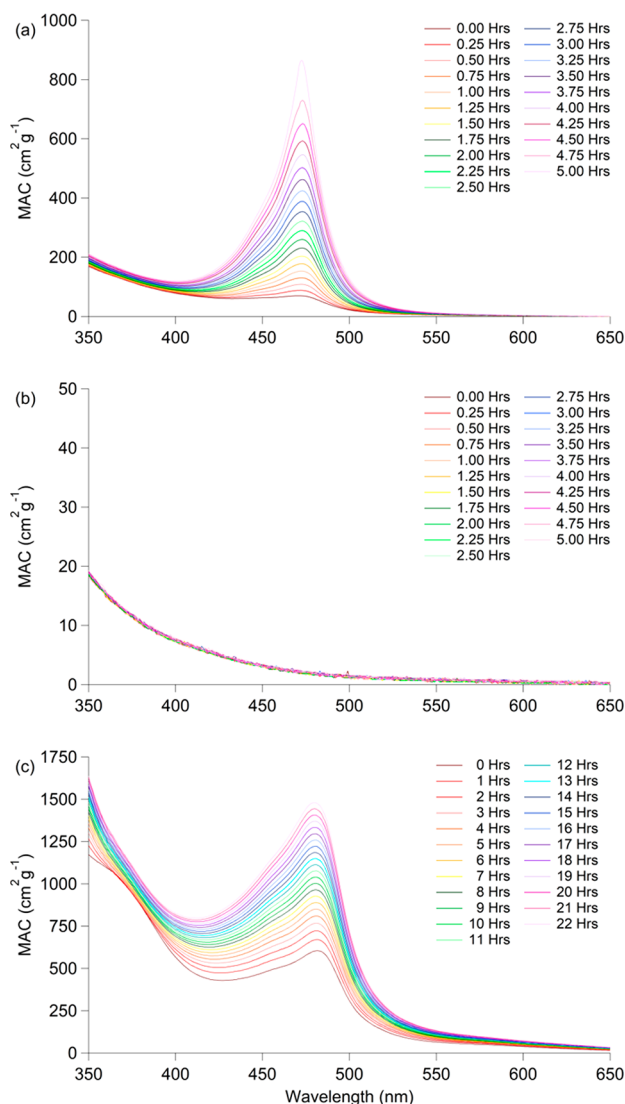


Figure 4. (a) MAC of 0.2 M 4-OPA in 0.1 M 2-MP versus time showing the growth of a peak at 475 nm. (b) MAC of 0.2 M 4-OPA in 0.1 M 1-MP over time showing no peak growth. (c) MAC of LSOA reacted with 0.1 M 2-MP with a peak growing at 482 nm. MAC was calculated using eq 1. Y-axis is scaled differently in each panel to show differences between each system.

under these reaction conditions. Under other reaction conditions, such as the heating described in the amine and amino acid section below, 1-MP may potentially lead to browning by a different chemical mechanism.

The experiments were also carried out for LSOA with 2-MP, in absence of NH_3 . Similarly to the 4-OPA + 2-MP mixtures, LSOA reaction with 0.1 M 2-MP resulted in efficient browning evidenced by the growth of a peak at 482 nm in the UV-vis spectrum (Figure 4c). At a similar mass concentration to 4-OPA, LSOA in 0.1 M 2-MP browned more slowly than 4-OPA. In the LSOA mixture only a fraction of species have the necessary structure for efficient browning, so the overall concentration of compounds capable of browning is lower compared to solutions containing only 4-OPA.

Collectively, these experiments confirm that the conversion of 4-OPA into 2-MP may be an important initial step in the browning process. They also suggest that similar pyrrole-based intermediates may be important in browning chemistry of

LSOA. The 2-MP absorbs only in the UV range, so it cannot be responsible for the brown color of the solution. However, oligomerization reactions involving 2-MP as an intermediate may produce more complex, conjugated compounds capable of absorbing visible radiation. A unique feature of the pyrrole ring is that nitrogen donates its nonbonding electrons to the ring by resonance. Increased electron density at C atoms makes them accessible for electrophilic substitution, such as reactions with aldehydes and ketones, with the C_5 carbon of the pyrrole ring being the most reactive (Figure 2). The presence of more than one reactive site in the 2-MP ring (C_3 , C_4 , C_5) and two carbonyl groups in 4-OPA provides multiple cross-oligomerization pathways that may lead to the formation of larger light-absorbing species. The molecular identity of the chromophores responsible for the appearance of the distinctive 475 nm absorption band in the 4-OPA + AS and 4-OPA + 2-MP is outside of the scope of this study, and will be discussed in detail in a follow-up publication.

3.2. Browning of 4-OPA Accelerated by Evaporation.

The mechanism outlined in Figure 2 suggests that the browning process may be accelerated by actively removing water from the 4-OPA + AS system. In the evaporation experiments, 0.1 M AS or AN was mixed with 0.06 M 4-OPA and the solution was evaporated. The reaction products were subsequently redissolved in water and the evaporation process was repeated until the change in MAC values was minimal between the successive evaporations. Figure 5 shows that the evaporation of 4-OPA + AS and 4-OPA + AN solutions resulted in MAC values comparable to those obtained in the much slower reaction in unevaporated aqueous solutions. The reaction appears to be very fast and limited by the evaporation rate. For example, a comparison of Figure 3 (MAC of $\sim 100 \text{ cm}^2 \text{ g}^{-1}$ achieved after about 24 h of aqueous reaction) and

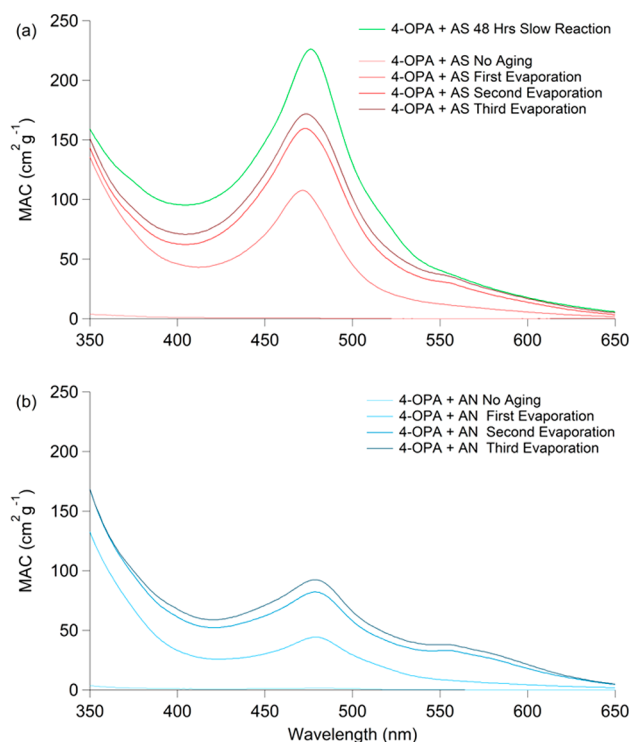


Figure 5. MAC after evaporation and dissolution for 0.1 M AS (a) and AN (b) reacting with 0.06 M 4-OPA. For the 4-OPA + AS case, the result of slow aging in aqueous unevaporated solution is also shown.

Figure 5 (MAC of $\sim 100 \text{ cm}^2 \text{ g}^{-1}$ achieved after 10 min in the first evaporation) suggests that BrC formation reactions occur at least 2–3 orders of magnitude faster during the evaporation process.

Figure 5 shows that the evaporation of AS yields a MAC value nearly two times higher than AN ($180 \text{ cm}^2 \text{ g}^{-1}$ for AS and $100 \text{ cm}^2 \text{ g}^{-1}$ for AN). The initial solution pH was very similar (5.2 in 0.1 M AS and 5.1 in 0.1 M AN based on the E-AIM model II: <http://www.aim.env.uea.ac.uk/aim/aim.php>).⁶³ However, the solution of AS has twice as many ammonium ions than AN, and the extent of browning occurring in the reaction with 4-OPA may be dependent on the total amount of ammonium ions present in the system. Additionally, AN is more likely to volatilize as $\text{HNO}_3 + \text{NH}_3$ during the evaporation process leaving less nitrogen available for the reaction. The absorption spectra are slightly different for the 4-OPA + AS and 4-OPA + AN cases: the 4-OPA + AN spectrum is slightly red-shifted and has more pronounced additional bands between 550 and 600 nm. This difference suggests that the anion also affects the structures of the products, possibly by altering the ionic strength and pH of the evaporating solution as well as solubility of 4-OPA. For example, glyoxal hydration equilibrium is known to be strongly and selectively affected by the sulfate anions;^{44,64} similar effects may occur for the hydration of 4-OPA. A control experiment was performed with 4-OPA in deionized water to examine the reactivity of 4-OPA undergoing evaporation in the absence of ammonium ions. This experiment did not result in the growth of any peaks in the MAC spectrum, confirming that the ammonium ions are needed for the browning.

The evaporation of 4-OPA + AS and 4-OPA + AN solutions resulted in smaller MAC values compared to MAC values after 48 h of reaction in unevaporated aqueous solution (Figure 5). In the previous studies of LSOA + AS⁴⁶ and glyoxal + AS,⁶⁵ the evaporation was found to produce larger MAC values than the slower aqueous reaction. It is possible that some 4-OPA was lost during the evaporation step because it is a fairly volatile molecule. Although the MAC values of the evaporated mixtures were somewhat lower, they may be more atmospherically relevant because they produce BrC at a much faster rate and are less likely to compete with the photobleaching of BrC by sunlight that has been observed in several studies.^{36,66}

3.3. Browning Reactions of 4-OPA Reacting with Amines and Amino Acids. In order to further explore the BrC-forming potential of 4-OPA, additional studies were conducted with 4-OPA reacted with a variety of nitrogen-containing organic compounds. The amines and amino acids produced visible browning of the solutions, but this was not the case for nitroso and amide compounds. The concentration and time dependence of the reaction was then further quantified by keeping the 4-OPA concentration constant and varying the concentration of the nitrogen-containing species. This generally shows that 4-OPA has the ability to react with these nitrogen-containing compounds and over time form products that have the ability to absorb in the UV and more importantly the visible region. This is not to say that these amines and amino acids react by the same mechanism as AS and 2-MP. For example, secondary and tertiary amines cannot undergo the intramolecular reaction shown in Figure 2 to form pyrrole structures. A possible pathway for brown carbon formation with secondary amines and 4-OPA is the production of an enamine followed by an intermolecular reaction with a second 4-OPA molecule, similar to a Stork enamine alkylation, leading

to oligomerization. Tertiary amines and 4-OPA can undergo aldol condensation reactions promoted by the basicity of the amines.

Figure 6 compares the MAC values after nine 75 min heating intervals (675 min; the concentration of all nitrogen-containing

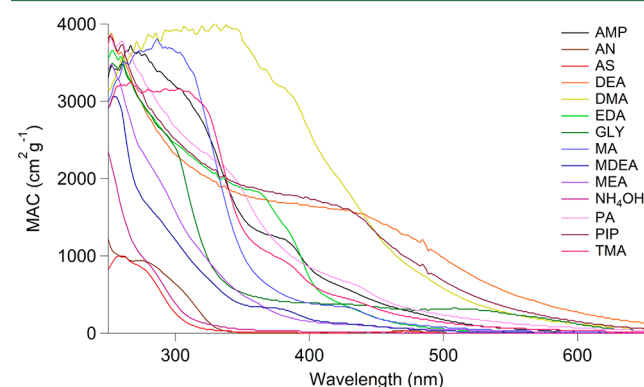


Figure 6. MAC after 675 min of aging at 40 °C. The concentration of 4-OPA was 0.015 M and the concentration of each nitrogen-containing compound was 0.035 M. Abbreviations of nitrogen-containing compounds: 2-amino-2-methyl-1-propanol (AMP), ammonium nitrate (AN), ammonium sulfate (AS), diethylamine (DEA), dimethylamine (DMA), ethylenediamine (EDA), glycine (GLY), methylamine (MA), methyldiethanolamine (MDEA), ethanolamine (MEA), ammonium hydroxide (NH_4OH), propylamine (PA), piperazine (PIP), and trimethylamine (TMA).

species is 0.035 M). In all cases, there is an increase in MAC values in the UV region with a broad absorption tail extending into the visible region. The largest MAC values in the visible range were observed for secondary amines DMA, DEA, and PIP. In several cases specific peaks are observed, such as for MA at 325 nm and for PA near 350 nm. The MAC values in the visible region were considerably larger for amines and amino acids compared to NH_4OH , AN, and AS, which have the lowest MAC values in Figure 6. The much larger MAC values resulting from reaction of amines and amino acids with 4-OPA can compensate for the fact that amines and amino acids are less abundant in the atmosphere compared to AS.

3.4. Atmospheric Implications. The experiments described in this paper demonstrate that 4-OPA may be the smallest atmospherically relevant molecule that undergoes browning by the same general mechanism as previously observed in LSOA. This assertion is based on the fact that browning of 4-OPA in an aqueous solution in the presence of AS produces remarkably similar absorption spectra to those observed for the LSOA + AS system. Furthermore, similar spectra are observed in reactions of 4-OPA with 2-MP and of LSOA with 2-MP, supporting the hypothesis that pyrrole-based compounds act as probable intermediates in this browning chemistry. Pyrroles are reactive toward carbonyls, and they may continue to react with 4-OPA or structurally related compounds in LSOA to produce larger, light-absorbing products. The MAC values from the 4-OPA + AS reaction products are modest, and not large enough to compete with primary BrC from biomass burning, but reactions of 4-OPA could provide important insights into the chemical mechanisms of secondary BrC formation in reactions of SOA. Although the aqueous reaction of 4-OPA with either AS or AN is relatively slow, it is greatly accelerated by condensation reactions promoted by evaporation. This reinforces the suggestion

from previous studies that BrC can be produced efficiently in evaporation of cloud and fog droplets. Finally, the browning of 4-OPA is not limited to reactions with AN and AS. It can also react with a variety of other nitrogen-containing species including amines, amino acids, and compounds containing ammonium ions. Of these, secondary amines produce the highest MAC values in the visible region. We conclude that 4-OPA is a convenient model system for studying secondary BrC formation in reactions of carbonyls and reduced nitrogen compounds.

AUTHOR INFORMATION

Corresponding Author

*Phone: (949) 824-1262; fax: (949) 824-2420; e-mail: nizkorod@uci.edu.

ORCID

Alexander Laskin: 0000-0002-7836-8417

Julia Laskin: 0000-0002-4533-9644

Sergey A. Nizkorodov: 0000-0003-0891-0052

Notes

The authors declare no competing financial interest.

ACKNOWLEDGMENTS

We acknowledge support by the U.S. Department of Commerce, National Oceanic and Atmospheric Administration through Climate Program Office's AC4 program, awards NA13OAR4310066, NA13OAR4310062. PA acknowledges support from the Ford Foundation Predoctoral Fellowship Program of the National Academy of Science and the NSF Graduate Research Fellowship Program. Some of the measurements were performed at the W.R. Wiley Environmental Molecular Sciences Laboratory (EMSL), a national scientific user facility located at PNNL, and sponsored by the Office of Biological and Environmental Research of the U.S. DOE. PNNL is operated for US DOE by Battelle Memorial Institute under Contract No. DEAC06-76RL0 1830.

REFERENCES

- (1) Boucher, O.; Randall, D.; Artaxo, P.; Bretherton, C.; Feingold, G.; Forster, P.; Kerminen, V. M.; Kondo, Y.; Liao, H.; Lohmann, U.; Rasch, P.; Sathesh, S. K.; Sherwood, S.; Stevens, B.; Zhang, X. Y. *Climate Change 2013: The Physical Science Basis. Contribution of Working Group I to the Fifth Assessment Report of the Intergovernmental Panel on Climate Change*; Cambridge University Press: New York, NY, 2013.
- (2) Climate Change 2007: The Physical Science Basis. Contribution of Working Group I to the Fourth Assessment Report of the Intergovernmental Panel on Climate Change. In *IPCC*, Solomon, S.; Qin, D.; Manning, M.; Chen, Z.; Marquis, M.; Averyt, K. B.; Tignor, M.; Miller, H. L., Eds.; Cambridge University Press: Cambridge, United Kingdom and New York, NY, USA, 2007.
- (3) Finlayson-Pitts, B. J.; Pitts, Jr, J. N. *Chemistry of the Upper and Lower Atmosphere: Theory, Experiments, and Applications*; Academic Press: San Diego, CA, 2000.
- (4) Forster, P.; Ramaswamy, V.; Artaxo, P.; Berntsen, T.; Betts, R.; Fahey, D. W.; Haywood, J.; Lean, J.; Lowe, D. C.; Myhre, G.; Nganga, J.; Prinn, R.; Raga, G.; Schulz, M.; Van Dorland, R.; Changes in Atmospheric Constituents and in Radiative Forcing. In *Climate Change 2007: The Physical Science Basis. Contribution of Working Group I to the Fourth Assessment Report of the Intergovernmental Panel on Climate Change*; Cambridge University Press: Cambridge, United Kingdom and New York, NY, 2007; pp 129–243.
- (5) Alexander, D. T.; Crozier, P. A.; Anderson, J. R. Brown carbon spheres in East Asian outflow and their optical properties. *Science* **2008**, *321* (5890), 833–36.
- (6) Andreae, M. O.; Gelencser, A. Black carbon or brown carbon? The nature of light-absorbing carbonaceous aerosols. *Atmos. Chem. Phys.* **2006**, *6* (10), 3131–48.
- (7) Bond, T. C.; Bergstrom, R. W. Light absorption by carbonaceous particles: an investigative review. *Aerosol Sci. Technol.* **2006**, *40* (1), 27–67.
- (8) Bahadur, R.; Praveen, P. S.; Xu, Y.; Ramanathan, V. Solar absorption by elemental and brown carbon determined from spectral observations. *Proc. Natl. Acad. Sci. U. S. A.* **2012**, *109* (43), 17366–71.
- (9) Chunga, C. E.; Ramanathan, V.; Decremera, D. Observationally constrained estimates of carbonaceous aerosol radiative forcing. *Proc. Natl. Acad. Sci. U. S. A.* **2012**, *109* (29), 11624–29.
- (10) Ramanathan, V.; Li, F.; Ramana, M. V.; Praveen, P. S.; Kim, D.; Corrigan, C. E.; Nguyen, H.; Stone, E. A.; Schauer, J. J.; Carmichael, G. R.; Adhikary, B.; Yoon, S. C. Atmospheric brown clouds: hemispherical and regional variations in long-range transport, absorption, and radiative forcing. *J. Geophys. Res.* **2007**, *112*, D22S21.
- (11) Usher, C. R.; Michel, A. E.; Grassian, V. H. Reactions on mineral dust. *Chem. Rev.* **2003**, *103* (12), 4883–4940.
- (12) Laskin, A.; Laskin, J.; Nizkorodov, S. A. Chemistry of atmospheric brown carbon. *Chem. Rev.* **2015**, *115* (10), 4335–82.
- (13) Moosmüller, H.; Chakrabarty, R. K.; Arnott, W. P. Aerosol light absorption and its measurement: a review. *J. Quant. Spectrosc. Radiat. Transfer* **2009**, *110* (11), 844–78.
- (14) Chang, J. L.; Thompson, J. E. Characterization of colored products formed during irradiation of aqueous solutions containing H₂O₂ and phenolic compounds. *Atmos. Environ.* **2010**, *44* (4), 541–51.
- (15) Gelencser, A.; Hoffer, A.; Kiss, G.; Tombacz, E.; Kurdi, R.; Bencze, L. In-situ formation of light-absorbing organic matter in cloud water. *J. Atmos. Chem.* **2003**, *45* (1), 25–33.
- (16) Hoffer, A.; Kiss, G.; Blazso, M.; Gelencser, A. Chemical characterization of humic-like substances (HULIS) formed from a lignin-type precursor in model cloud water. *Geophys. Res. Lett.* **2004**, *31*, L06115.
- (17) Lin, Y. H.; Budisulistiorini, S. H.; Chu, K.; Siejack, R. A.; Zhang, H.; Riva, M.; Zhang, Z.; Gold, A.; Kautzman, K. E.; Surratt, J. D. Light-absorbing oligomer formation in secondary organic aerosol from reactive uptake of isoprene epoxydiols. *Environ. Sci. Technol.* **2014**, *48* (20), 12012–21.
- (18) Limbeck, A.; Kulmala, M.; Puxbaum, H. Secondary organic aerosol formation in the atmosphere via heterogeneous reaction of gaseous isoprene on acidic particles. *Geophys. Res. Lett.* **2003**, *30* (19), 1996.
- (19) Rincon, A. G.; Guzmán, M. I.; Hoffmann, M. R.; Colussi, A. J. Optical absorptivity versus molecular composition of model organic aerosol matter. *J. Phys. Chem. A* **2009**, *113* (39), 10512–20.
- (20) Rincon, A. G.; Guzmán, M. I.; Hoffmann, M. R.; Colussi, A. J. Thermochromism of model organic aerosol matter. *J. Phys. Chem. Lett.* **2010**, *1* (1), 368–73.
- (21) Casale, M.; Richman, A.; Elrod, M.; Garland, R.; Beaver, M.; Tolbert, M. Kinetics of acid-catalyzed aldol condensation reactions of aliphatic aldehydes. *Atmos. Environ.* **2007**, *41* (29), 6212–24.
- (22) Noziere, B.; Esteve, W. Light-absorbing aldol condensation products in acidic aerosols: spectra, kinetics, and contribution to the absorption index. *Atmos. Environ.* **2007**, *41* (6), 1150–63.
- (23) Esteve, W.; Noziere, B. Uptake and reaction kinetics of acetone, 2-butanone, 2,4-pentanedione, and acetaldehyde in sulfuric acid solutions. *J. Phys. Chem. A* **2005**, *109* (48), 10920–28.
- (24) Garland, R. M.; Elrod, M. J.; Kincaid, K.; Beaver, M. R.; Jimenez, J. L.; Tolbert, M. A. Acid-catalyzed reactions of hexanal on sulfuric acid particles: identification of reaction products. *Atmos. Environ.* **2006**, *40* (35), 6863–78.
- (25) Krizner, H. E.; De Haan, D. O.; Kua, J. Thermodynamics and kinetics of methylglyoxal dimer formation: a computational study. *J. Phys. Chem. A* **2009**, *113* (25), 6994–7001.

- (26) Noziere, B.; Esteve, W. Organic reactions increasing the absorption index of atmospheric sulfuric acid aerosols. *Geophys. Res. Lett.* **2005**, *32*, L03812.
- (27) Noziere, B.; Voisin, D.; Longfellow, C. A.; Friedli, H.; Henry, B. E.; Hanson, D. R. The uptake of methyl vinyl ketone, methacrolein, and 2-methyl-3-butene-2-ol onto sulfuric acid solutions. *J. Phys. Chem. A* **2006**, *110* (7), 2387–95.
- (28) Zhao, J.; Levitt, N. P.; Zhang, R. Heterogeneous chemistry of octanal and 2,4-hexadienal with sulfuric acid. *Geophys. Res. Lett.* **2005**, *32*, L09802.
- (29) Jacobson, M. Z. Isolating nitrated and aromatic aerosols and nitrated aromatic gases as sources of ultraviolet light absorption. *J. Geophys. Res.* **1999**, *104* (D3), 3527–42.
- (30) Kwamena, N. O. A.; Abbatt, J. P. D. Heterogeneous nitration reactions of polycyclic aromatic hydrocarbons and n-hexane soot by exposure to NO₃/NO₂/N₂O₅. *Atmos. Environ.* **2008**, *42* (35), 8309–14.
- (31) Pitts, J. N., Jr.; Van Cauwenberghe, K. A.; Grosjean, D.; Schmid, J. P.; Fitz, D. R.; Belser, W. L., Jr.; Knudson, G. B.; Hynds, P. M. Atmospheric reactions of polycyclic aromatic hydrocarbons: facile formation of mutagenic nitro derivatives. *Science* **1978**, *202* (4367), 515–19.
- (32) Song, C.; Gyawali, M.; Zaveri, R. A.; Shilling, J. E.; Arnott, W. P. Light absorption by secondary organic aerosol from α -pinene: effects of oxidants, seed aerosol acidity, and relative humidity. *J. Geophys. Res. Atmos.* **2013**, *118*, 11741–49.
- (33) Powelson, M. H.; Espelien, B. M.; Hawkins, L. N.; Galloway, M. M.; De Haan, D. O. Brown carbon formation by aqueous-phase carbonyl compound reactions with amines and ammonium sulfate. *Environ. Sci. Technol.* **2014**, *48* (2), 985–93.
- (34) Lin, P.; Laskin, J.; Nizkorodov, S. A.; Laskin, A. Revealing brown carbon chromophores produced in reactions of methylglyoxal with ammonium sulfate. *Environ. Sci. Technol.* **2015**, *49* (24), 14257–66.
- (35) Tang, M.; Alexander, J. M.; Kwon, D.; Estilloro, A. D.; Laskina, O.; Young, M. A.; Kleiber, P. D.; Grassian, V. H. Optical and physicochemical properties of brown carbon aerosol: light scattering, FTIR extinction spectroscopy, and hygroscopic growth. *J. Phys. Chem. A* **2016**, *120* (24), 4155–66.
- (36) Zhao, R.; Lee, A. K. Y.; Huang, L.; Li, X.; Yang, F.; Abbatt, J. P. D. Photochemical processing of aqueous atmospheric brown carbon. *Atmos. Chem. Phys.* **2015**, *15* (11), 6087–6100.
- (37) Galloway, M. M.; Chhabra, P. S.; Chan, A. W. H.; Surratt, J. D.; Flagan, R. C.; Seinfeld, J. H.; Keutsch, F. N. Glyoxal uptake on ammonium sulphate seed aerosol: reaction products and reversibility of uptake under dark and irradiated conditions. *Atmos. Chem. Phys.* **2009**, *9* (10), 3331–45.
- (38) Noziere, B.; Dziedzic, P.; Cordova, A. Products and kinetics of the liquid-phase reaction of glyoxal catalyzed by ammonium ions (NH₄⁺). *J. Phys. Chem. A* **2009**, *113* (1), 231–37.
- (39) Sareen, N.; Schwier, A. N.; Shapiro, E. L.; Mitroo, D.; McNeill, V. F. Secondary organic material formed by methylglyoxal in aqueous aerosol mimics. *Atmos. Chem. Phys.* **2010**, *10* (3), 997–1016.
- (40) De Haan, D. O.; Tolbert, M. A.; Jimenez, J. L. Atmospheric condensed-phase reactions of glyoxal with methylamine. *Geophys. Res. Lett.* **2009**, *36*, L11819.
- (41) Shapiro, E. L.; Szprengiel, J.; Sareen, N.; Jen, C. N.; Giordano, M. R.; McNeill, V. F. Light-absorbing secondary organic material formed by glyoxal in aqueous aerosol mimics. *Atmos. Chem. Phys.* **2009**, *9* (7), 2289–2300.
- (42) Trainic, M.; Abo Riziq, A.; Lavi, A.; Flores, J. M.; Rudich, Y. The optical, physical and chemical properties of the products of glyoxal uptake on ammonium sulfate seed aerosols. *Atmos. Chem. Phys.* **2011**, *11* (18), 9697–9707.
- (43) Kampf, C. J.; Jakob, R.; Hoffmann, T. Identification and characterization of aging products in the glyoxal/ammonium sulfate system - implications for light-absorbing material in atmospheric aerosols. *Atmos. Chem. Phys.* **2012**, *12* (14), 6323–33.
- (44) Yu, G.; Bayer, A. R.; Galloway, M. M.; Korshavn, K. J.; Fry, C. G.; Keutsch, F. N. Glyoxal in aqueous ammonium sulfate solutions: products, kinetics and hydration effects. *Environ. Sci. Technol.* **2011**, *45* (15), 6336–42.
- (45) Bones, D. L.; Henricksen, D. K.; Mang, S. A.; Gonsior, M.; Bateman, A. P.; Nguyen, T. B.; Cooper, W. J.; Nizkorodov, S. A. Appearance of strong absorbers and fluorophores in limonene-O₃ secondary organic aerosol due to NH₄⁺-mediated chemical aging over long time scales. *J. Geophys. Res.* **2010**, *115*, D05203.
- (46) Nguyen, T. B.; Lee, P. B.; Updyke, K. M.; Bones, D. L.; Laskin, J.; Laskin, A.; Nizkorodov, S. A. Formation of nitrogen- and sulfur-containing light-absorbing compounds accelerated by evaporation of water from secondary organic aerosols. *J. Geophys. Res.* **2012**, *117*, D01207.
- (47) Updyke, K. M.; Nguyen, T. B.; Nizkorodov, S. A. Formation of brown carbon via reactions of ammonia with secondary organic aerosols from biogenic and anthropogenic precursors. *Atmos. Environ.* **2012**, *63*, 22–31.
- (48) Lee, H. J.; Laskin, A.; Laskin, J.; Nizkorodov, S. A. Excitation-emission spectra and fluorescence quantum yields for fresh and aged biogenic secondary organic aerosols. *Environ. Sci. Technol.* **2013**, *47* (11), 5763–70.
- (49) Flores, J. M.; Washenfelder, R. A.; Adler, G.; Lee, H. J.; Segev, L.; Laskin, J.; Laskin, A.; Nizkorodov, S. A.; Brown, S. S.; Rudich, Y. Complex refractive indices in the near-ultraviolet spectral region of biogenic secondary organic aerosol aged with ammonia. *Phys. Chem. Chem. Phys.* **2014**, *16* (22), 10629–42.
- (50) Laskin, J.; Laskin, A.; Roach, P. J.; Slysz, G. W.; Anderson, G. A.; Nizkorodov, S. A.; Bones, D. L.; Nguyen, L. Q. High-resolution desorption electrospray ionization mass spectrometry for chemical characterization of organic aerosols. *Anal. Chem.* **2010**, *82* (5), 2048–58.
- (51) Laskin, J.; Laskin, A.; Nizkorodov, S. A.; Roach, P.; Eckert, P.; Gilles, M. K.; Wang, B.; Lee, H. J.; Hu, Q. Molecular selectivity of brown carbon chromophores. *Environ. Sci. Technol.* **2014**, *48* (20), 12047–55.
- (52) Nguyen, T. B.; Laskin, A.; Laskin, J.; Nizkorodov, S. A. Brown carbon formation from ketoaldehydes of biogenic monoterpenes. *Faraday Discuss.* **2013**, *165*, 473–94.
- (53) Kampf, C. J.; Filippi, A.; Zuth, C.; Hoffmann, T.; Opatz, T. Secondary brown carbon formation via the dicarbonyl imine pathway: nitrogen heterocycle formation and synergistic effects. *Phys. Chem. Chem. Phys.* **2016**, *18* (27), 18353–64.
- (54) Fruekilde, P.; Hjorth, J.; Jensen, N. R.; Kotzias, D.; Larsen, B. Ozonolysis at vegetation surfaces: a source of acetone, 4-oxopentanal, 6-methyl-5-hepten-2-one, and geranyl acetone in the troposphere. *Atmos. Environ.* **1998**, *32* (11), 1893–1902.
- (55) Forester, C. D.; Wells, J. R. Yields of carbonyl products from gas-phase reactions of fragrance compounds with OH radical and ozone. *Environ. Sci. Technol.* **2009**, *43* (10), 3561–68.
- (56) Matsunaga, S.; Michihiro, M.; Kimitaka, K. Variation on the atmospheric concentrations of biogenic carbonyl compounds and their removal processes in the northern forest at Moshiri, Hokkaido Island in Japan. *J. Geophys. Res.* **2004**, *109*, D04302.
- (57) Matsunaga, S.; Mochida, M.; Kawamura, K. High abundance of gaseous and particulate 4-oxopentanal in the forestal atmosphere. *Chemosphere* **2004**, *55* (8), 1143–47.
- (58) Helmig, D.; Pollock, W.; Greenberg, J.; Zimmerman, P. Gas chromatography mass spectrometry analysis of volatile organic trace gases at Mauna Loa Observatory, Hawaii. *J. Geophys. Res.* **1996**, *101* (D9), 14697–710.
- (59) Ciccioli, P.; Brancaleoni, E.; Frattoni, M.; Cecinato, A.; Brachetti, A. Ubiquitous occurrence of semi-volatile carbonyl compounds in tropospheric samples and their possible sources. *Atmos. Environ., Part A* **1993**, *27* (12), 1891–1901.
- (60) Anderson, S. E.; Franko, J.; Jackson, L. G.; Wells, J. R.; Ham, J. E.; Meade, B. J. Irritancy and allergic responses induced by exposure to the indoor air chemical 4-oxopentanal. *Toxicol. Sci.* **2012**, *127* (2), 371–81.
- (61) Weschler, C. J.; Wisthaler, A.; Cowlin, S.; Tamás, G.; Ström-Tejse, P.; Hodgson, A. T.; Destaillets, H.; Herrington, J.; Zhang, J.

Nazaroff, W. W. Ozone-initiated chemistry in an occupied simulated aircraft cabin. *Environ. Sci. Technol.* **2007**, *41* (17), 6177–84.

(62) Chen, Y.; Bond, T. C. Light absorption by organic carbon from wood combustion. *Atmos. Chem. Phys.* **2010**, *10* (4), 1773–87.

(63) Friese, E.; Ebel, A. Temperature dependent thermodynamic model of the system H^+ - NH_4^+ - Na^+ - SO_4^{2-} - NO_3^- - Cl^- - H_2O . *J. Phys. Chem. A* **2010**, *114* (43), 11595–11631.

(64) Kampf, C. J.; Waxman, E. M.; Slowik, J. G.; Dommen, J.; Pfaffenberger, L.; Praplan, A. P.; Prévôt, A. S. H.; Baltensperger, U.; Hoffmann, T.; Volkamer, R. Effective Henry's law partitioning and the salting constant of glyoxal in aerosols containing sulfate. *Environ. Sci. Technol.* **2013**, *47* (9), 4236–44.

(65) Lee, A. K.; Zhao, R.; Li, R.; Liggio, J.; Li, S. M.; Abbatt, J. P. Formation of light absorbing organo-nitrogen species from evaporation of droplets containing glyoxal and ammonium sulfate. *Environ. Sci. Technol.* **2013**, *47* (22), 12819–26.

(66) Lee, H. J.; Aiona, P. K.; Laskin, A.; Laskin, J.; Nizkorodov, S. A. Effect of solar radiation on the optical properties and molecular composition of laboratory proxies of atmospheric brown carbon. *Environ. Sci. Technol.* **2014**, *48* (17), 10217–26.